

ARTICLES

 0° polarization transfer in ${}^2\text{H}(\vec{p}, \vec{n})pp$ at 54 and 71 MeV

M. A. Pickar,* S. Burzynski,[†] C. Gysin, M. Hammans, R. Henneck, J. Jourdan,
W. Lorenzon, and I. Sick
Institut für Physik, University of Basel, CH-40506 Basel, Switzerland

A. Berdoz[‡] and F. Foroughi[§]
Institute de Physique, Université de Neuchâtel, CH-40000 Neuchâtel, Switzerland
(Received 11 July 1989; revised manuscript received 11 April 1990)

Results of measurements of the transverse polarization transfer coefficients $K_y^{y'}(0^\circ)$ for ${}^2\text{H}(\vec{p}, \vec{n})pp$ at 54 and 71 MeV are presented. The magnitude and energy dependence of this parameter have been determined with sufficient precision (4%) to permit the use of this reaction as a source of nearly monoenergetic polarized neutrons in precise measurements. $K_y^{y'}(0^\circ)$ is found to have a significant dependence on excitation energy. The results at low excitation energy are in agreement with calculations in the impulse approximation using the nucleon-nucleon phase shifts obtained from the Bonn or Paris potentials. A substantial difference from the results obtained using the empirical phase shifts is found. Results of measurements of the longitudinal polarization transfer coefficient $K_z^z(0^\circ)$ at 54 MeV are also presented.

I. INTRODUCTION

A better determination of the neutron-proton interaction, particularly the tensor component, remains an important goal in nuclear physics. Measurements of polarization observables, particularly spin-correlation observables, provide an effective means of probing aspects of the nucleon-nucleon force that would be almost impossible by any other means.^{1,2} Such studies require polarized beams and polarized targets. The absolute determination of the polarization of the beams and targets is often the largest source of error in such measurements. A substantial investment must be made in calibrating such beams and targets before significant advances can be made in our determination of the nucleon-nucleon force.

This paper describes our measurements of the polarization transfer coefficients $K_y^{y'}(0^\circ)$ and $K_z^z(0^\circ)$ for the neutron production reaction ${}^2\text{H}(\vec{p}, \vec{n})pp$.^{3,4} The polarized neutrons produced in this reaction have been used to measure the spin-correlation parameter $A_{zz}(\theta)$ for elastic np scattering at 68 MeV.^{1,2} A_{zz} provides a unique tool to extract the 3S_1 - 3D_1 mixing parameter ϵ_1 , which can be directly related to the isoscalar NN tensor force. An additional motivation to investigate $K_y^{y'}$ and K_z^z stems from the fact that these observables in themselves yield information on the nucleon-nucleon force.

The reaction ${}^2\text{H}(\vec{p}, \vec{n})pp$ previously has been used to produce polarized neutron beams only at high energy.⁵⁻⁹ At energies near 50 MeV the reaction ${}^2\text{H}(\vec{d}, \vec{n}){}^3\text{He}$ has been routinely used up to now.^{10,11} The disadvantage of this reaction is the large flux of lower energy neutrons. Although these neutrons can be used effectively in some measurements, in high-precision measurements of spin-

correlation observables, where the polarized target is primarily a heavy contaminant material, it is desirable to have a monoenergetic beam. Such a beam minimizes systematic errors arising, for example, from background subtraction. In addition, systematic errors in measurements with a longitudinally polarized beam tend to be minimized if the beam is monoenergetic, as the contribution of transverse components is reduced. A monoenergetic beam also minimizes extraneous rate in the detection apparatus, permitting one to run with significantly higher neutron flux in the peak region.

Although the reaction ${}^2\text{H}(\vec{p}, \vec{n})pp$ produces a neutron spectrum at 0° that is almost monoenergetic, the peak one observes is the result of the strong 1S_0 final-state interaction of the two protons,¹² and not that of a transition to a bound final state. As a result, the neutron polarization is not just a number, but rather a *function* of excitation energy. There have been previous studies of this energy dependence,¹³⁻¹⁶ but none sufficiently precise for our application. At lower bombarding energies (~ 15 MeV) (Refs. 13 and 14) the polarization transfer is a strong function of excitation energy, while at higher energies (~ 160 MeV) (Ref. 15) the functional dependence becomes relatively weak. In a preliminary investigation of this reaction¹⁶ we found that the variation of polarization transfer with excitation energy is significant, but not as strong as that observed at lower energies. Data available for the average value of the polarization transfer^{17,18} near energies of interest to us are insufficient. In the work to be described, we attained the necessary precision by making measurements of high statistical accuracy, with good experimental resolution, and with the effects contributing to the resolution well enough determined so as to permit

an accurate unfolding of the intrinsic polarization transfer function.

II. EXPERIMENTAL METHOD

A. The beam line

The measurements were made using the low-energy polarized neutron source at the Paul Scherrer Institute (PSI).¹⁹ This facility has been described in detail elsewhere,^{3,4} so only the essentials of it will be discussed here.

Polarized protons are produced in an atomic-beam-type polarized ion source and accelerated to energies as high as 72 MeV by the Injector I cyclotron. Beams of 1 μA and 85% polarization are typically produced. Beam bursts of width 0.7 ns, separated by 20 ns, are obtained at 72 MeV, increasing to about 1.2 ns, separated by 70 ns, at 55 MeV.

The beam is guided to area NE-C, which contains the neutron source (Fig. 1). Upon entering the area, the beam passes through an in-beam polarimeter (POL), which is used to monitor the polarization of the beam continuously.²⁰ The device consists of a thin carbon foil ($200 \mu\text{g}/\text{cm}^2$) viewed by two small NaI detectors placed symmetrically, left and right, at the peak of the analyzing power ($\sim 45^\circ$). Using precise analyzing powers from the literature,^{21,22} this device provides a determination of the normal component of the proton beam polarization good to 1% absolute.²³ A small NaI detector was also placed above the beam at 45° for use in measurements of the longitudinal polarization transfer. A small plastic scintillator, called the "timing scintillator," is positioned below the polarimeter target at 30° . This detector provides an effective means of monitoring the beam timing relative to the cyclotron rf and of the microscopic time structure of the beam bursts.

The beam is guided to the production target ($T1$) by a dipole magnet ($D1$) and a pair of quadrupoles (Q). The charged particles exiting the target are swept aside into a Faraday cup (FC) by a dipole magnet ($D2$). $D2$ also provides the necessary precession of the neutron spin in the measurements of the longitudinal polarization transfer.⁴

The production target $T1$ is liquid deuterium (LD_2)

operating at about 19 K and 1 atm. The region through which the beam passes is 1.1 cm thick. The design of the target is such that it permits the use of proton beams at 72 MeV with intensities as high as 5 μA with almost no decrease in density.³ The energy loss of 72 MeV protons in this target is ~ 2.0 MeV.

The neutrons exit the production target to pass through a collimator at 0° . The collimator was such as to produce a beam 4.2 cm diameter at the neutron target position $T2$ (422 cm from the production target). The use of neutrons at 0° permits a rapid reversal in the polarization direction of the neutrons by flipping the orientation of the proton polarization in the atomic source. The neutron source is surrounded on all sides by iron and concrete shielding.

In the measurements of transverse polarization transfer, the direction of polarization (N) of the incoming protons and outgoing neutrons was not affected by the beam line elements. This was not the case in the measurements of the longitudinal polarization transfer.⁴ Here, a solenoid (SOL) was placed just before the in-beam polarimeter and set to precess the proton polarization to be in the plane of the L - R pair of detectors, i.e., an S polarized beam was formed at that point. Deflecting the beam by 54° in $D1$ then resulted in an almost completely (97.7%) longitudinally polarized beam (L). The longitudinal spin component of the high-energy peak neutrons was then precessed 90° by $D2$ to produce neutrons polarized in the S direction. This polarization component could then be analyzed with our apparatus (see below) rotated 90° about the beam axis.⁴

B. The measurement apparatus

The apparatus used to measure the polarization of the beam in the case of transverse polarization transfer is illustrated in Fig. 1. The setup for the case of longitudinal polarization transfer was virtually identical, except for a 90° rotation about the axis of the neutron beam.⁴

The reaction used to measure the neutron beam polarization was elastic scattering from ${}^4\text{He}$. The large analyzing powers, A_j , the amount of precise data available for ${}^4\text{He}(\vec{p}, p){}^4\text{He}$ in our energy range,^{24,25} and the connection

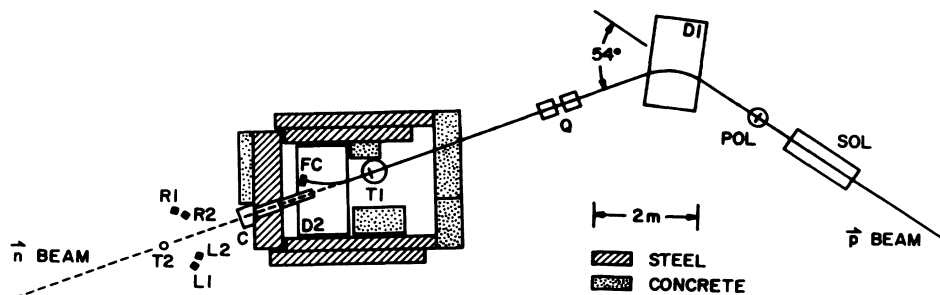


FIG. 1. Schematic of the PSI low-energy polarized neutron facility and the experimental setup showing the principal components: spin precession solenoid (SOL), proton polarimeter (POL), bending magnets ($D1, D2$), quadrupoles (Q), liquid deuterium neutron production target ($T1$), Faraday cup (FC), neutron collimator (C), liquid helium scattering target ($T2$), and neutron detectors ($L1, L2, R1, R2$).

to ${}^4\text{He}(\bar{n}, n){}^4\text{He}$ via charge symmetry, make ${}^4\text{He}$ a suitable choice as an analyzer. An additional benefit is a clean event identification. This results from the use of the material as an active target and because it has its first excited state at 20.1 MeV of excitation.

This technique has been used in determining the polarization of neutron beams at lower energy.²⁶⁻²⁷ Neutron beam polarization at higher energies has without exception been analyzed via np elastic scattering and the results of phase-shift analyses. The absolute precision to which the polarization of such beams can be determined thus depends to a large extent on how well the analyzing powers for np scattering can be determined from measured observables other than A_y . Our neutron beam will thus supply the means of obtaining the highest energy data for spin observables in np scattering with independent calibration.

Our target (T_2) was liquid helium at 4 K and 1 atm contained in a 50 mm inside diameter, flattened sphere made of Pyrex with 1.1 mm walls.²⁸ The inner walls were coated with a wavelength shifter. Except for the flattened portion on the bottom of the target container, the outer walls were coated with a reflective white paint. The scintillation photons from the liquid helium exited the flattened bottom portion of the container to enter a Plexiglas light guide spaced about 1 cm away. This pipe was connected to a photomultiplier tube. To minimize the material in the beam and to reduce multiple scattering effects in the outside walls, the glass bulb was surrounded only by several layers of superinsulation and a thin-walled (0.5 mm) aluminum cylinder of diameter 10 cm.

The scattered neutrons were detected in two pairs of detectors positioned symmetrically about the neutron beam (L1, L2, R1, and R2 in Fig. 1). Each detector consisted of two bars of NE102 plastic scintillator, each 4.1 cm thick \times 10.0 cm wide \times 50.0 cm high. Each bar was coupled via a light pipe to a single 7.6 cm photomultiplier tube. The bars were tilted 22° relative to the vertical so as to compensate for the dispersion in pulse arrival times for interactions at different points along the height of the detector.²⁹ The neutron detectors were positioned 70 cm from the helium target at several angles near the maximum analyzing power ($\sim 130^\circ_{\text{lab}}$).

During the experiment the following information was recorded event-by-event on magnetic tape: the pulse height in the active target (α pulse height), the time-of-flight (TOF) of the pulse observed in the active target relative to the cyclotron rf (α -rf TOF), the pulse height observed in the neutron detector (n pulse height), and the time-of-flight of the neutron detector pulse relative to the target pulse (α - n TOF). Spin state was flipped about once a minute. At each spin flip scalars were also written to magnetic tape. These included charge into the Faraday cup, pulser triggers (used in making dead-time corrections), and rates in various detectors. For each run the proton beam polarization was monitored continuously, and the polarimeter spectra were recorded. The timing of the proton beam relative to the cyclotron rf was also monitored continuously via the rf "timing scintillator" spectrum.

III. DATA REDUCTION

The data for each detector, at each angle and each spin state, were sorted with various restrictive cuts applied on the input signal sources. A threshold was set on the neutron pulse height to reduce the random background. Sorts made with different thresholds produced results identical to within the statistical errors.

With cuts on neutron pulse height and α -rf TOF, a clear peak was visible in the α pulse-height spectrum. A cut was made on the α pulse height to reduce background from inelastic scattering on helium, and other sources.

With the above cuts applied, the spectrum for α - n TOF consisted of a sharp peak corresponding to the elastically scattered neutrons, sitting on a small and flat background. A cut on this peak was used to better define the events of interest in the other three signal sources.

A representative set of spectra after all cuts have been applied is illustrated in Fig. 2. The α pulse-height spectrum has a width of about 12%, chiefly due to the nonuniformity of response throughout the active target. The α -rf TOF spectrum has a FWHM of 1.7 ns arising from contributions from the intrinsic width of the neutron beam (0.6 ns), the width of the proton beam burst (0.8 ns), the time spread due to finite target size (0.6 ns), and the time resolution of the active target (0.6 ns). The spectrum for α - n TOF has a sharp peak with a width of 1.1 ns, arising primarily from the resolutions of the α detector (0.6 ns) and the n detector (0.8 ns).

The yields were obtained by integrating the peak in the α - n TOF and subtracting the underlying background, obtained by making a linear fit to the regions on either side of the peak region. These yields were corrected for dead time and normalized to the incident proton charge in the Faraday cup. The dead time was obtained by injecting a random pulser obtained from the "timing scintillator." This pulser system also made it possible to continuously record the time structure of the beam and drifts in the rf relative to the beam.

For a given bin in the α -rf TOF spectrum asymmetries were calculated via

$$\epsilon_L = \frac{Y_L^\uparrow - Y_L^\downarrow}{Y_L^\uparrow + Y_L^\downarrow}, \quad (1)$$

$$\epsilon_R = \frac{Y_R^\downarrow - Y_R^\uparrow}{Y_R^\downarrow + Y_R^\uparrow} \quad (2)$$

for the single arms, and for the super ratio, ϵ_S , where,

$$\epsilon_S = \frac{1-r}{1+r} \quad (3)$$

$$r = \left[\frac{Y_L^\uparrow \times Y_R^\downarrow}{Y_L^\downarrow \times Y_R^\uparrow} \right]^{1/2}. \quad (4)$$

Here Y_L^\uparrow (Y_R^\downarrow) corresponds to the yield in the left (right) detector for an incident proton polarized with spin direction up (down). The asymmetries obtained using the various combinations of the yields agreed to within their statistical uncertainties. The result obtained using the super-ratio method was that used in the final analysis, as

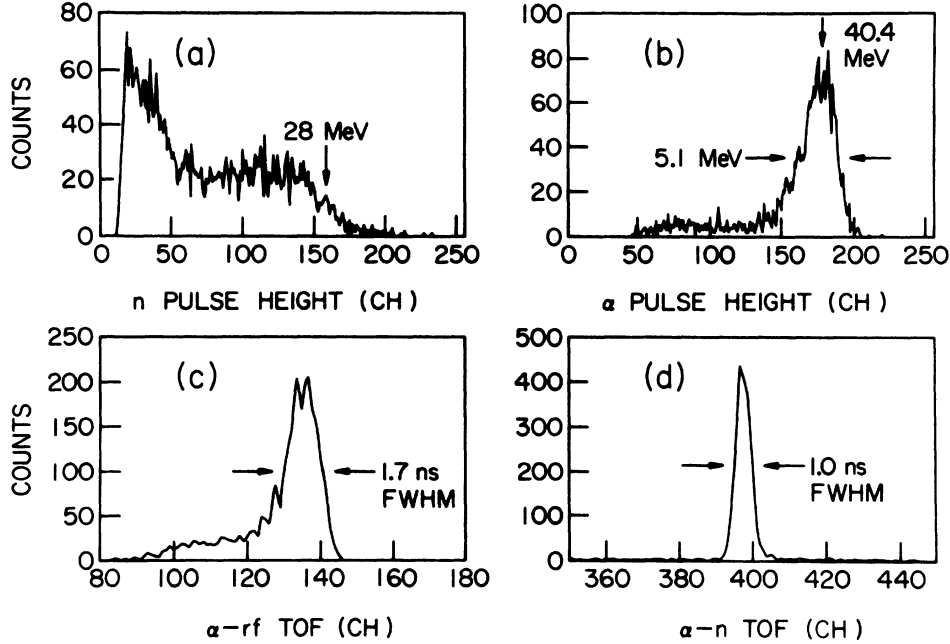


FIG. 2. Representative set of spectra after all cuts have been applied: (a) n pulse height; (b) α pulse height; (c) α -rf TOF; (d) α - n TOF. These results were obtained using incident neutrons with a mean energy of 67.5 MeV, and a laboratory scattering angle of 145° .

it effectively reduced some of the systematic uncertainties present in the other two procedures

IV. DATA ANALYSIS AND RESULTS

In the limit of a monoenergetic neutron beam, a point target, and point neutron detectors, the transverse polarization of the neutron beam is obtained from the expression

$$P_n = \frac{\epsilon}{A_y(\theta)}, \quad (5)$$

where $A_y(\theta)$ is the analyzing power for ${}^4\text{He}(\bar{n}, n){}^4\text{He}$ at the angle θ . The transverse polarization transfer coefficient $K_y^{y'}(0^\circ)$ is obtained from the proton transverse polarization P_p and the neutron transverse polarization P_n via

$$P_n = K_y^{y'}(0^\circ)P_p. \quad (6)$$

For the case of longitudinal polarization transfer we get the equivalent⁴

$$K_z^{z'} = \frac{\epsilon}{P_p A_y(\theta)}, \quad (7)$$

where P_p is now the proton longitudinal polarization.

The elementary relationships in Eqs. (5)–(7) cannot be directly utilized in the real experiment. We have assumed knowledge of A_y for ${}^4\text{He}(\bar{n}, n){}^4\text{He}$, when in fact that information is not *directly* available. There is, however, an appreciable body of experimental data available for ${}^4\text{He}(\bar{p}, p){}^4\text{He}$, from which phase shifts can be obtained.^{25,30} Charge symmetry tells us that aside from “small” Coulomb corrections, the phase shifts, and observables, for ${}^4\text{He}(\bar{n}, n){}^4\text{He}$ and ${}^4\text{He}(\bar{p}, p){}^4\text{He}$ should be

identical. Since these are five-nucleon systems, approximations must be made in order to evaluate the Coulomb corrections. For the tightly bound ${}^4\text{He}$ system, the effective two-body treatment of Coulomb distortions presented by Fröhlich *et al.*³¹ is expected to provide a close description of the true distortions. This model has been quantitatively tested in the case of π^\pm - ${}^{16}\text{O}$ elastic scattering,³² and for N - ${}^4\text{He}$ elastic scattering at 24 MeV.³³ In both cases excellent agreement was obtained.

In this model the full scattering amplitude includes the pure hadronic term, a relativistic point Coulomb term, a Coulomb term accounting for the finite extension of the projectile and the target, and a piece originating from the interference between the Coulomb and hadronic interactions. Detailed calculations for N - ${}^4\text{He}$ using the Saito phase shifts³⁰ demonstrate that at the energies of interest to this work, the effect of the relativistic point Coulomb term on the analyzing power (typically less than 4%) is almost canceled by the contributions of the remaining Coulomb distortion effects when one is in the vicinity of the maximum of A_y , occurring at back angles.³⁴

In other words, in the region of the maximum of A_y , at back angles, we expect the analyzing powers for elastic neutron scattering from ${}^4\text{He}$ to be almost identical to those for elastic proton scattering from ${}^4\text{He}$.

Calculations performed between 50 and 65 MeV,³⁴ using the Saito phase shifts,³⁰ have led us to the conclusion that the assumption that the peak $p\alpha$ analyzing powers are the same as the peak $n\alpha$ analyzing powers is good to 3%. The calculations yield peak $n\alpha$ analyzing powers that differ from peak $p\alpha$ values by +0.001 at 50 MeV, by -0.008 at 52 MeV, and by +0.021 at 59 MeV. Two significantly different results were obtained at 65 MeV, due to the larger uncertainties in the energy dependence of the phase shifts. The preferred result, using phases in

better agreement with a more recent phase shift analysis,²⁵ differs from $p\alpha$ by -0.016 , and the other by -0.044 . In all cases the maximum analyzing powers for $p\alpha$ exceed $+0.90$.

In addition to accurate analyzing powers, extraction of intrinsic polarization transfer coefficients from our data requires a number of geometric corrections to be made. The target is sufficiently large that multiple scattering effects must also be incorporated.³⁵ The multiple scattering corrections can be grouped into two categories; those involving only the liquid helium itself (MS1), and those in which one has at least one scattering with the enclosing walls (MS2). Since our target is active, and we make a cut on target pulse height, the multiple scattering events affecting our measurements are only those producing α 's of the requisite energy in the active volume. Heavy recoils from the enclosing walls rarely penetrate to the active volume, and those that do produce a negligible amount of light. As a result, events in category MS2 are dominated by a small-angle scattering in the walls, and a large-angle scattering in the active volume.

The necessary geometric corrections for finite size, MS1, and MS2, were obtained by performing Monte Carlo calculations in which the experimental geometry and reduction cuts were incorporated. Calculations were performed for various detector angles and various neutron energies. In this manner an array of geometric correction factors, $\delta(T_n, \theta_{\text{det}})$, was obtained. From this an array of effective analyzing powers, $A_y'(T_n, \theta_{\text{det}})$, could be constructed, where

$$A_y'(T_n, \theta_{\text{det}}) = \frac{A_y(T_n, \theta_{\text{det}})}{1 + \delta(T_n, \theta_{\text{det}})}, \quad (8)$$

and A_y was the analyzing power for point detectors and no multiple scattering. Table I illustrates the size of these corrections for a neutron energy of 67.5 MeV and a detector at various angles near the peak of A_y' . Using this information one may then compute the average polarization transfer coefficient, $\overline{K_y^{y'}}$, for a given bin of the α -rf TOF.

As pointed out earlier, the problem of predicting the analyzing powers for ${}^4\text{He}(n, n){}^4\text{He}$ using the phase shifts from ${}^4\text{He}(p, p){}^4\text{He}$ leads to uncertainties of about 3% in

the absolute magnitude of the analyzing power near its maximum.³⁴ It also leads to an uncertainty of a few degrees in the angle at which that maximum occurs. We have used the results obtained at different angles to obtain the angular shift. In Fig. 3 we see the experimentally determined values of A_y' at a mean neutron energy $\overline{T_n} = 67.5$ MeV. We observe the data to be shifted forward $1.5^\circ \pm 0.5^\circ$. At the lower energy ($\overline{T_n} = 50.8$ MeV) we find the data to be shifted backward $2.0^\circ \pm 0.5^\circ$. We applied these shifts to the data to obtain the appropriate angle at which to evaluate the function A_y' . Using these factors we then obtained mean values of $\overline{K_y^{y'}}$ (bin). In Figs. 4 and 5 we give the results for mean proton energies $\overline{T_p}$ of 54.5 and 71.4 MeV, respectively.

In Fig. 6 are illustrated the results obtained for $\overline{K_z^{z'}}$ (bin), the longitudinal polarization transfer, at $\overline{T_p} = 54.1$ MeV. The results at higher excitation were subject to sizable corrections because those lower energy neutrons were precessed more than the neutrons in the peak for which the dipole ($D2$) was set. Further corrections had to be made for the contributions arising from a transverse component in the incident proton beam polarization.

The data points in Figs. 4–6 are plotted at the mean neutron energy of each bin, with the bin size indicated by the spacing between the points. Also shown is the average value obtained with a wide cut, corresponding to an average over the first three bins in each spectrum.

These preliminary results indicate a significant variation of $\overline{K_y^{y'}}$, and neutron beam polarization, with outgoing neutron energy. Because the neutron yield is also a pronounced function of outgoing neutron energy [see the dash-dot-dashed curves in Figs. 4(b), 5(b), and 6(b)] and the cross section for neutron-alpha elastic scattering varies rapidly with bombarding energy, the effects of experimental energy resolution become an important concern in extracting the intrinsic distribution.

In this experiment, the energy of the incident neutron was determined by a time-of-flight (TOF) measurement using the signal from the active target and the cyclotron rf. Factors directly affecting the time resolution include the uncertainty in the flight path of the neutron due to the extended size of the production and active targets (~ 0.6 ns), the time response of the active target (~ 0.6 ns), and the time structure of the proton beam burst

TABLE I. A sample of some of the geometric corrections applied to the data for an incident neutron energy of 67.5 MeV. FG refers to finite geometry corrections alone. MS1 refers to corrections arising from multiple scattering within the liquid helium. MS2 refers to multiple scattering corrections involving one scattering from the material surrounding the helium. Total is the sum of all corrections. A_y is the analyzing power for point target and point detector, and A_y' is the effective analyzing power incorporating the geometric corrections.

θ_{det} (deg)	Corrections (%)				Total	A_y	A_y'
	FG	MS1	MS2	Total			
120	13.5	1.0	0.6	15.1	0.423	0.367	
125	10.0	1.6	1.6	13.2	0.809	0.715	
130	6.6	1.6	1.5	9.7	0.983	0.896	
135	3.8	1.3	1.3	6.4	0.946	0.889	
140	2.1	1.0	1.0	4.1	0.829	0.796	
145	1.3	0.8	0.8	2.9	0.698	0.678	
150	0.9	0.7	0.6	2.2	0.576	0.563	

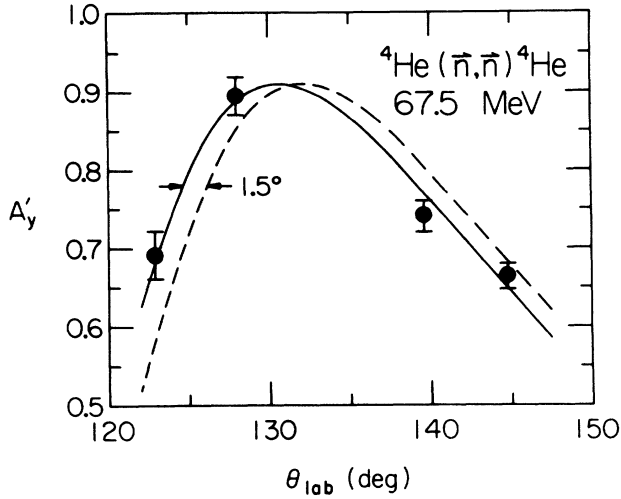


FIG. 3. Experimentally determined values of A'_y (●) at a mean neutron energy $\bar{T}_n = 67.5$ MeV compared to the predicted results (dashed curve) for A'_y in ${}^4\text{He}(n, n){}^4\text{He}$, obtained from the ${}^4\text{He}(p, p){}^4\text{He}$ phase shifts. The solid curve illustrates the fitted results obtained by shifting the dashed curve forward 1.5° . These analyzing powers A'_y include the effects of finite geometry and multiple scattering, and are not to be confused with the intrinsic analyzing powers A_y .

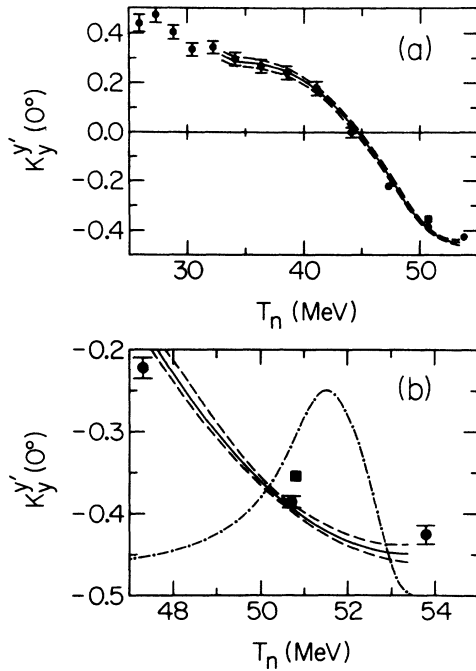


FIG. 4. The results of a preliminary analysis of the data for $K_y^{y'}(0^\circ)$, incorporating corrections for finite geometry and multiple scattering, at a mean proton energy of 54.5 MeV are indicated by the data points (●) in (a) and (b). Part (b) is an expanded view of the region at low excitation. The average over the first three data regions is indicated by ■. The vertical bar represents the statistical error. The solid curve represents the results of the final analysis, incorporating corrections for energy resolution, with the one-sigma region of statistical uncertainty bounded by the dashed curves. There is an additional systematic error of 4%. In (b) the dash-dot-dashed curve shows the intrinsic distribution of the incident neutron flux.

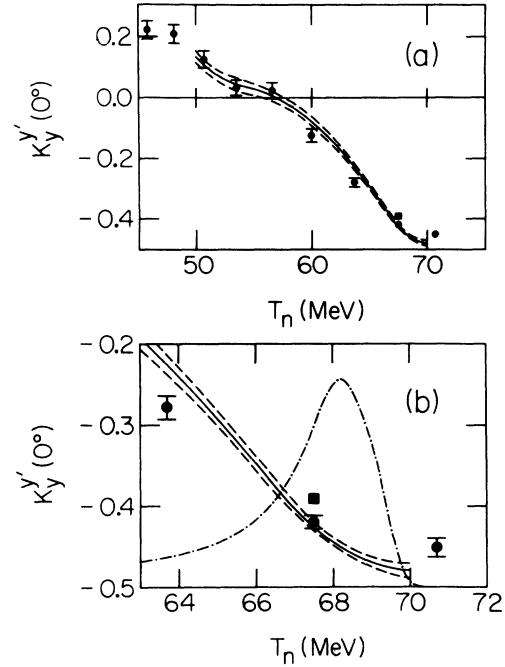


FIG. 5. The same as Fig. 4, but for $K_y^{y'}(0^\circ)$ at a mean proton energy of 71.4 MeV.

(FWHM ≈ 0.6 – 1.4 ns). These combine to give a typical resolution of ~ 1.4 ns. This is to be compared to neutron flight times of ~ 40 ns for 67 MeV neutrons.

These resolution functions can be used to extract the intrinsic time distributions of $K_y^{y'}$ and $K_z^{z'}$, and hence their energy distributions. The method used was a fitting procedure incorporating Monte Carlo techniques. The

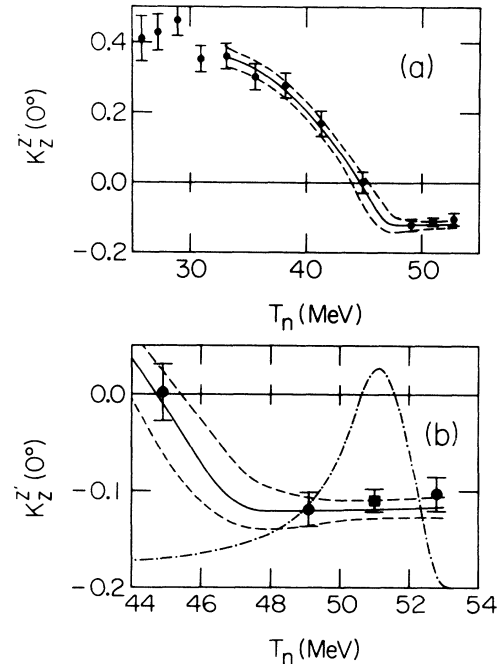


FIG. 6. The same as Fig. 4, but for $K_z^{z'}(0^\circ)$ at a mean proton energy of 54.1 MeV.

intrinsic energy distribution of neutrons from the production target was obtained from an independent measurement with far better energy resolution (0.5 MeV).

For the energy dependence of $K_y^{y'}$ and $K_z^{z'}$ we assumed a simple function of neutron energy with the following form:

$$K = a_1 + b_1x + c_1x^3, \quad 0 \leq x < x_1 \quad (9)$$

$$K = a_2 + b_2x + c_2x^2, \quad x_1 \leq x < x_2 \quad (10)$$

$$K = a_3 + b_3x + c_3x^2, \quad x_2 \leq x < x_3 \quad (11)$$

where x denotes $T - T_{\max}$ which is identically equal to the "excitation energy," T denotes the neutron kinetic energy, and T_{\max} denotes the maximum neutron kinetic energy.

The function is assumed to be continuous and differentiable at the boundaries x_1 and x_2 . This results in a fit to seven parameters. In all the fits there was no significant evidence for values of b_1 significantly different from zero. Since the yield in the first region is strongly dominated by the transition ${}^3S_1 \rightarrow {}^1S_0$, we also expect K to be almost a constant there. Thus, b_1 was fixed to zero, resulting in a fit to only six parameters; a_1, c_1, c_2, c_3, x_1 , and x_2 .

For each iteration of the fitting procedure, the whole experiment was simulated and symmetries within a time bin α calculated via

$$\epsilon_\alpha^* = \frac{\int K A_y' \sigma' f}{\int \sigma' f}, \quad (12)$$

where f denotes the weight functions for the neutron flux, σ' denotes the neutron-alpha cross section, A_y' denotes the neutron-alpha analyzing power, and K denotes the polarization transfer coefficient.

The final results of the fits for $K_y^{y'}$ and $K_z^{z'}$ are listed in Table II. A comparison of these corrected polarization transfer coefficients to those from the preliminary

analysis can be seen in Figs. 4–6. The final values are represented by the solid curves, with the "one-sigma" regions of statistical uncertainty bounded by the dashed curves.

In the vicinity of the observed peak of the scattered neutron flux this uncertainty is minimum, having a value of $\sim 1.5\%$. Note that this occurs at an energy about 1 MeV higher in excitation than the energy at which the bombarding neutron flux peaks. This is a result of the rapid increase in cross section as the neutron energy decreases.

There is a systematic uncertainty of 4.0% arising from the combination of a 3% uncertainty in the absolute analyzing power for ${}^4\text{He}(\bar{n}, n){}^4\text{He}$,³⁴ a 1% uncertainty in the absolute proton beam polarization,^{20–23} and an estimated 2% uncertainty from the analysis procedure. One should note that the absolute uncertainty in the proton beam polarization does not contribute to the systematic uncertainty in the neutron beam polarization.

V. DISCUSSION

A. Comparison to existing data

When one compares the average transverse polarization transfer in the peak region to other measurements made in our energy range,^{17,18} the results of this experiment are found to be more negative. In Fig. 7 are shown our final corrected results at 0 MeV excitation, and when averaged over 3 MeV and 10 MeV of excitation energy. We see a significant change in the results when increasing the energy range over which the average is made. The 50, 60, and 80 MeV data of Sakai *et al.*¹⁸ result from an average over ~ 6 MeV, and the 30 and 50 MeV data of Robertson *et al.*,¹⁷ from an average over ~ 5 MeV. These groups did not correct their results for the resolution of their apparatus.

Robertson *et al.*,¹⁷ use a method similar to ours, but the necessary corrections to their results are significantly

TABLE II. Results of the full analysis yielding the parameters used to describe the variation of the polarization transfer coefficients with excitation energy (see the text for details). The curves resulting from these parameters can be found in Figs. 4–6. The indicated uncertainties are statistical. There is an additional systematic error of 4%.

Parameter	$K_y^{y'}$ (71 MeV)	$K_y^{y'}$ (54 MeV)	$K_z^{z'}$ (54 MeV)
T_p (MeV)	72.4	55.7	55.3
\bar{T}_p (MeV)	71.4	54.5	54.1
T_n^{peak} (MeV)	68.2	51.1	50.7
T_n^{max} (MeV)	70.1	53.4	53.1
a_1	-0.48004	-0.44848	-0.11620
b_1	+0.00000	+0.00000	-0.00181
c_1	+0.00784	+0.00740	+0.00020
c_2	-0.00213	-0.00306	+0.01597
c_3	+0.00386	+0.00641	-0.00188
x_1 (MeV)	3.778	5.364	5.329
x_2 (MeV)	15.99	18.24	7.12
K (Excitation=0 MeV)	-0.4800±0.0130	-0.4485±0.0110	-0.1164±0.0130
\bar{K} (3 MeV excitation)	-0.4511±0.0054	-0.4212±0.0048	-0.1186±0.0075
\bar{K} (10 MeV excitation)	-0.3964±0.0068	-0.3550±0.0062	-0.1096±0.0120

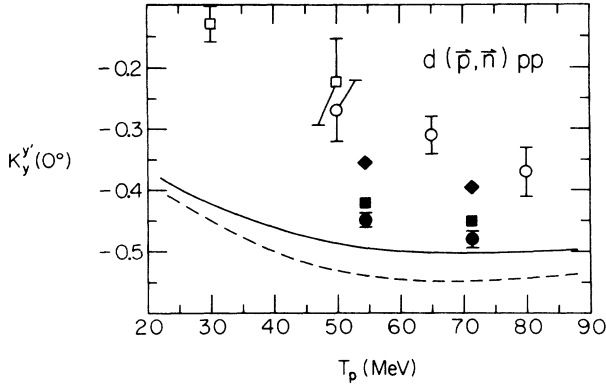


FIG. 7. Average values of $K_y^{y'}(0^\circ)$. The data are from Ref. 17 (\square) and Ref. 18 (\circ); the results of this work are for an average over 3 MeV (\blacksquare) and 10 MeV (\blacklozenge) of excitation, and in the limit of no excitation (\bullet). The indicated errors are statistical. There is an additional 4% systematic error in the results of this work. The solid curve is the prediction in the impulse approximation using the Bonn (Ref. 42) and Paris (Ref. 43) phase shifts. The dashed curve is the result using the empirical phase shifts of Arndt *et al.* (Refs. 44 and 45).

greater than those of this work. We have made a rough estimate of these corrections and find their corrected results to be roughly comparable with the present work.

Another possible source of the lack of agreement is in the analyzing powers of the reaction used to determine the neutron beam polarization. Sakai *et al.*¹⁸ use 0° neutrons from the ${}^6\text{Li}(\bar{p}, \bar{n}){}^6\text{Be}$ (0^+ state) reaction,³⁶ with the polarization of the neutrons assumed to be identical to that of the protons from the analog reaction ${}^6\text{Li}(\bar{p}, \bar{p}'){}^6\text{Be}^*$ (0^+ state). This equality is expected to hold if one assumes charge independence. This assumption is far more restrictive than the one made in our study, where we merely assumed charge symmetry, and imposed realistic Coulomb corrections.

The results of our study of the longitudinal transfer coefficient, $K_z^{z'}$, provide the only data for that observable for the reaction ${}^2\text{H}(\bar{p}, \bar{n})pp$ below 500 MeV. Although this quantity is found to be large at energies between 500 and 800 MeV,^{8,9} at 54 MeV it is found to be quite small (~ -0.1).

This is actually expected as, for a reaction with the spin structure $1 + \frac{1}{2} \rightarrow 0 + \frac{1}{2}$, one finds the following identity to hold at 0° :³⁷

$$K_z^{z'} + 2K_y^{y'} = -1. \quad (13)$$

This applies to ${}^2\text{H}(\bar{p}, \bar{n})pp$ to the extent that we can neglect the D state of the deuteron, and that the two final-state protons are in the 1S_0 configuration. Corrections for these effects have been shown to amount to less than 3% at low excitation.³⁸⁻⁴⁰ We find at 54 MeV,

$$\begin{aligned} (-0.1164 \pm 0.013) + 2(-0.4485 \pm 0.011) \\ = -1.013 \pm 0.026. \quad (14) \end{aligned}$$

The excellent agreement with the expectation is considered a very important check on the internal consistency

of our results, particularly for the absolute normalization of the $n\alpha$ analyzing powers used in the analysis.

B. Comparison to calculations

Exact calculations of breakup observables in the three-nucleon system are possible, in principle, using the Faddeev equations, but are in practice very difficult to perform. Calculations that have been made restrict themselves to low bombarding energies and to relatively simple approximations of the nucleon-nucleon interaction. In addition, no realistic calculation has been performed which includes the Coulomb potential.

At the energies of interest to this experiment, one expects calculations based on the impulse approximation to become valid. As noted by Phillips,¹² an S state is strongly favored at low excitation for the final proton-proton state. Since the D state of the deuteron is small and has little effect on the interaction at low excitation energies, one may assume a pure S -wave deuteron wave function. In this approximation one can then compute the polarization transfer coefficient directly from the nucleon-nucleon phase shifts.³⁸⁻⁴⁰ Following Sakai *et al.*,^{15,18} one obtains for the ${}^2\text{H}(p, n)pp$, ${}^3S_1 \rightarrow {}^1S_0$ transition at 0° ,

$$K_y^{y'}(0^\circ) = \frac{-|F|^2}{2|B|^2 + |F|^2}, \quad (15)$$

where B and F are simply related to the spin-dependent central and tensor parts of the n - p scattering amplitude.⁴¹

Given this connection, one possibly can use $K_y^{y'}(0^\circ)$ as a means of distinguishing between potential models.^{12,17,18,38-40} Of particular interest is the sensitivity of $K_y^{y'}(0^\circ)$ to the tensor part of the np interaction.¹⁸ Before one can use the new information from the three-nucleon system to test the input from the two-nucleon system, one must first determine the degree of uncertainty incurred by the approximations made in this model. Phillips³⁸ estimates that the biggest uncertainty comes from the use of the impulse approximation, and that this amounts to $\sim 15\%$ at 40 MeV and $\sim 5\%$ at 150 MeV. More quantitative calculations^{15,39,40} of the necessary corrections yield much smaller results. We therefore expect the predicted values of $K_y^{y'}(0^\circ)$ in this approximation to be good to ± 0.03 in the limit of low excitation.

We have computed $K_y^{y'}(0^\circ)$ in this model using the phase shifts from the Bonn⁴² and Paris⁴³ potentials, obtained using the program SAID of Arndt and Roper.⁴⁴ Because the results are nearly identical, they are both represented by the solid curve in Fig. 7. Using the same program, we have also performed calculations using the empirical phase shifts obtained by Arndt *et al.*,^{44,45} yielding the dashed curve in Fig. 7.

Prior to this work, the available data^{17,18} were in poor agreement with the results of calculations using realistic potentials. One finds, however, that the new data are in good agreement with such calculations. The primary difference between these sets of data is in the resolution achieved and in the resolution corrections imposed, as discussed earlier in this paper.

One also notes in Fig. 7 that there is a significant

difference between the predictions of what are presently considered realistic potential models (Bonn⁴² and Paris⁴³), and the predictions employing the empirical phase shifts as determined by Arndt *et al.*⁴⁵ The origin of this difference can be attributed in large part to the ϵ_1 phase-shift mixing parameter.¹⁸ Because of the well-known correlation between 1P_1 and ϵ_1 in phase-shift analyses of the present np data base,^{46,47} we have investigated the sensitivity of $K_y^{y'}(0^\circ)$ to both 1P_1 and ϵ_1 . We find that the sensitivity to ϵ_1 is much greater than that to 1P_1 .

In way of illustration, if we increase ϵ_1 from its empirical value⁴⁵ of 1.0° at 70 MeV to 2.0° , a value consistent with the Paris and Bonn potentials, $K_y^{y'}$ changes from -0.55 to -0.52 . Changing 1P_1 from its empirical value of -8.1° at 70 MeV to -13.0° , a value consistent with the Paris and Bonn potentials, results in a change of $K_y^{y'}$ from -0.55 to -0.54 . The Paris and Bonn potentials yield values of -0.50 . At our highest energy, 71.4 MeV, we obtain a value of -0.480 in the limit of no excitation, with an absolute uncertainty of ± 0.019 . This is in good agreement with the predictions based on the potential models, but in significant disagreement with the predictions based on the empirical phase shifts.

VI. CONCLUSION

We have measured the transverse polarization transfer coefficients $K_y^{y'}(0^\circ)$ for ${}^2\text{H}(\vec{p}, \vec{n})pp$ at 54 and 71 MeV. The results vary rapidly with excitation energy, being large

and negative (~ -0.46) at low excitation and becoming positive within 13 MeV of excitation. The quantity has been determined with sufficient precision to permit a calculation of the effective neutron beam polarization for a variety of experiments to an absolute precision of 4%.

The longitudinal polarization transfer coefficients $K_z^z(0^\circ)$ have also been measured at 54 MeV. They are found to be small and negative (~ -0.1) at low excitation, and to become positive within 10 MeV of excitation. In the limit of low excitation our results are consistent with the expectation for a $\frac{1}{2} + 1 \rightarrow 0 + \frac{1}{2}$ spin transition.

The transverse polarization transfer coefficient, $K_y^{y'}(0^\circ)$, has been shown to be sensitive, at low excitation, to the tensor part of the np interaction. Our new data are in good agreement with the predictions made in an impulse approximation using modern nucleon-nucleon potentials. They are in significant disagreement with predictions based on empirical phase shifts. This difference can be attributed in large part to the mixing parameter ϵ_1 , which affords a direct means of probing the tensor force in the np system.

ACKNOWLEDGMENTS

This work was supported in part by the Swiss National Science Foundation. One of us (M.A.P.) also wishes to acknowledge support provided by the National Science Foundation under Grant No. NSF-EPSCoR Award RII-86-10671.

*Present address: Department of Physics and Astronomy, University of Kentucky, Lexington, KY 40506.

†Present address: Institute for Nuclear Studies, Hoza 69, Warsaw, Poland.

‡Present address: TRIUMF, 4004 Wesbrook Mall, Vancouver, British Columbia, V6T 2A3, Canada.

§Present address: Paul Scherrer Institute, CH-5234 Villigen, Switzerland.

¹M. A. Pickar, R. Henneck, C. Gysin, M. Hammans, W. Lorenzon, I. Sick, and S. Burzynski, *The Three-Body Force in the Three-Nucleon System*, Vol. 260 of *Lecture Notes in Physics*, edited by B. L. Berman and B. F. Gibson (Springer-Verlag, Berlin, 1986), p. 168.

²R. Henneck, J. Campbell, C. Gysin, M. Hammans, W. Lorenzon, M. A. Pickar, I. Sick, J. A. Konter, S. Mango, B. van den Brandt, and S. Burzynski, in *Intersections Between Particle and Nuclear Physics*, Proceedings of a Conference held in Rockport, ME, 1988, AIP Conf. Proc. **176**, edited by Gerry M. Bunce (AIP, New York, 1988), p. 1108.

³R. Henneck, C. Gysin, M. Hammans, J. Jourdan, W. Lorenzon, M. A. Pickar, I. Sick, S. Burzynski, and T. Stammach, Nucl. Instrum. Methods Phys. Res. **A259**, 329 (1987).

⁴R. Henneck, C. Gysin, P. Haffter, M. Hammans, W. Lorenzon, M. A. Pickar, I. Sick, and S. Burzynski, Phys. Rev. C **37**, 2224 (1988).

⁵J. Sowinski, R. C. Byrd, W. W. Jacobs, S. E. Vigdor, C. Whiddon, S. W. Wissink, L. D. Knutson, and P. L. Jolivet, Phys. Lett. B **199**, 341 (1987).

⁶R. Abegg, J. Birchall, E. Cairns, H. Coombes, C. A. Davis, N.

E. Davison, P. W. Green, L. G. Greeniaus, H. P. Gubler, W. P. Lee, W. J. McDonald, C. A. Miller, G. A. Moss, G. R. Plattner, P. R. Poffenberger, G. Roy, J. Soukup, J. P. Svenne, R. Tkachuk, W. T. H. van Oers, and Y. P. Zhang, Nucl. Instrum. Methods Phys. Res. **A234**, 11 (1985).

⁷C. Amsler, R. C. Brown, D. V. Bugg, J. A. Edgington, C. Oram, D. Axen, R. Dubois, L. Felawka, S. Jaccard, R. Keeler, J. Vavra, A. Clough, D. Gibson, G. A. Ludgate, N. M. Stewart, L. P. Robertson, and J. Reginald Richardson, Nucl. Instrum. Methods **144**, 401 (1977).

⁸P. J. Riley, C. L. Hollas, C. R. Newsom, R. D. Ransome, B. E. Bonner, J. E. Simmons, T. S. Bhatia, G. Glass, J. C. Hiebert, L. C. Northcliffe, and W. B. Tippens, Phys. Lett. **103B**, 313 (1981).

⁹J. S. Chalmers, W. R. Ditzler, T. Shima, H. Shimizu, H. Spinaka, R. Stanek, D. Underwood, R. Wagner, A. Yokosawa, J. E. Simmons, G. Burleson, C. Fontenla, T. S. Bhatia, G. Glass, and L. C. Northcliffe, Phys. Lett. **153B**, 235 (1985).

¹⁰F. N. Rad, R. G. Graves, D. P. Saylor, M. L. Evans, E. P. Chamberlain, J. W. Watson, and L. C. Northcliffe, Nucl. Instrum. Methods **190**, 459 (1981).

¹¹H. O. Klages, H. Dobiasch, P. Doll, H. Krupp, M. Oexner, P. Plischke, B. Zeitnitz, F. P. Brady, and J. C. Hiebert, Nucl. Instrum. Methods Phys. Res. **219**, 269 (1984).

¹²R. J. N. Phillips, Nucl. Phys. **53**, 650 (1964).

¹³P. W. Lisowski, R. C. Byrd, R. L. Walter, and T. B. Clegg, Nucl. Phys. **A334**, 45 (1980).

¹⁴R. G. Graves, Mahavir Jain, H. D. Knox, E. P. Chamberlain, and L. C. Northcliffe, Phys. Rev. Lett. **35**, 917 (1975).

- ¹⁵H. Sakai, T. A. Carey, J. B. McClelland, T. N. Taddeucci, R. C. Byrd, C. D. Goodman, D. Krofcheck, L. J. Rybarczyk, E. Sugarbaker, A. J. Wagner, and J. Rapaport, Phys. Rev. C **35**, 344 (1987).
- ¹⁶C. Gysin, M. Hammans, R. Henneck, J. Jourdan, W. Lorenzon, M. A. Pickar, I. Sick, A. Berdoz, F. Foroughi, C. Nussbaum, and S. Burzynski, J. Phys. Soc. Jpn. Suppl. **55**, 868 (1986).
- ¹⁷L. P. Robertson, R. C. Hanna, K. Ramavataram, D. W. Devins, T. A. Hodges, Z. J. Moroz, S. J. Hoey, and D. J. Plummer, Nucl. Phys. **A134**, 545 (1969).
- ¹⁸H. Sakai, N. Matsuoka, T. Saito, A. Shimizu, M. Tosaki, M. Ieiri, K. Imai, A. Sakaguchi, and T. Motobayashi, Phys. Lett. **B 177**, 155 (1986).
- ¹⁹This facility was previously named the Swiss Institute for Nuclear Physics (SIN).
- ²⁰C. Gysin, Diploma thesis, University of Basel, 1983.
- ²¹M. Ieiri, H. Sakaguchi, M. Nakamura, H. Sakamoto, H. Ogawa, M. Yosoi, T. Ichihara, N. Isshiki, Y. Takeuchi, H. Togawa, T. Tsutsumi, S. Hirata, T. Noro, and H. Ikegami, Nucl. Instrum. Methods Phys. Res. **A257**, 253 (1987).
- ²²S. Kato, K. Okada, M. Kondo, A. Shimizu, K. Hosono, T. Saito, N. Matsuoka, S. Nagamachi, K. Nisimura, N. Tamura, K. Imai, K. Egawa, M. Nakamura, T. Noro, H. Shimizu, K. Ogino, and Y. Kadota, Nucl. Instrum. Methods **169**, 589 (1980).
- ²³A very recent series of precise measurements of A_y for proton-carbon scattering by P. D. Eversheim *et al.* (unpublished), will provide a calibration of the in-beam polarimeter (POL) used in this work to *better* than 1% absolute at 71.2 MeV (R. Henneck, private communication).
- ²⁴K. Imai, K. Hatanaka, H. Shimizu, N. Tamura, K. Egawa, K. Nisimura, T. Saito, H. Sato, and Y. Wakuta, Nucl. Phys. **A325**, 397 (1979).
- ²⁵S. Burzynski, J. Campbell, M. Hammans, R. Henneck, W. Lorenzon, M. A. Pickar, and I. Sick, Phys. Rev. C **39**, 56 (1989).
- ²⁶R. L. York, J. C. Hiebert, H. L. Woolverton, and L. C. Northcliffe, Phys. Rev. C **27**, 46 (1983).
- ²⁷H. Krupp, J. C. Hiebert, H. O. Klages, P. Doll, J. Hansmeyer, P. Plischke, and J. Wilczynski, Phys. Rev. C **30**, 1810 (1984).
- ²⁸A. Berdoz, Ph.D. thesis, University of Lausanne, Switzerland, 1986.
- ²⁹C. D. Goodman, J. Rapaport, D. E. Bainum, and C. E. Brient, Nucl. Instrum. Methods **151**, 125 (1978); C. D. Goodman, J. Rapaport, D. E. Bainum, M. B. Greenfield, and C. A. Goulding, IEEE Trans. Nucl. Sci. **NS25**, 577 (1979).
- ³⁰T. Saito, Nucl. Phys. **A331**, 477 (1979).
- ³¹J. Fröhlich, H. Kriesche, L. Streit, and H. Zankel, Nucl. Phys. **A384**, 97 (1982).
- ³²J. Fröhlich, H. G. Schlaile, L. Streit, and H. Zingl, Z. Phys. A **302**, 89 (1981).
- ³³J. Fröhlich, Z. Phys. A **302**, 275 (1981).
- ³⁴H. Zankel, private communication.
- ³⁵S. Burzynski and R. Henneck, J. Phys. Soc. Jpn. Suppl. **55**, 888 (1986).
- ³⁶H. Sakai, N. Matsuoka, T. Noro, T. Saito, A. Shimizu, M. Tosaka, M. Ieiri, K. Imai, A. Sakaguchi, Y. Takeuchi, and T. Motobayashi, Nucl. Instrum. Methods Phys. Res. **A257**, 279 (1987).
- ³⁷G. G. Ohlsen, Rep. Prog. Phys. **34**, 717 (1972).
- ³⁸R. J. N. Phillips, Proc. Phys. Soc. London **74**, 652 (1959).
- ³⁹K. Ramavataram and Q. Ho-Kim, Nucl. Phys. **A156**, 395 (1970).
- ⁴⁰C. V. Dass and N. M. Queen, J. Phys. A **1**, 259 (1968).
- ⁴¹J. M. Moss, Phys. Rev. C **26**, 727 (1982).
- ⁴²R. Machleidt, K. Holinde, and Ch. Elster, Phys. Rep. **149**, 1 (1987).
- ⁴³M. Lacombe, B. Loiseau, J. M. Richard, R. Vinh Mau, J. Côté, P. Pirès, and R. de Tourreil, Phys. Rev. C **21**, 861 (1980).
- ⁴⁴R. A. Arndt and L. D. Roper, Scattering Analyses Interactive Dial-in (SAID) program, phase-shift solution SM86, Virginia Polytechnic Institute & State University (unpublished).
- ⁴⁵R. A. Arndt, J. S. Hyslop, III, and L. D. Roper, Phys. Rev. D **35**, 128 (1987).
- ⁴⁶J. Binstock and R. Bryan, Phys. Rev. D **9**, 2528 (1974).
- ⁴⁷D. V. Bugg, J. Phys. G **6**, 1329 (1980).